

Improved Solvation Models using Boundary Integral Equations

Matthew Knepley and Jaydeep Bardhan

Computational and Applied Mathematics
Rice University

Applied Mathematics Colloquium
Department of Mathematics
UNC Chapel Hill September 16, 2016



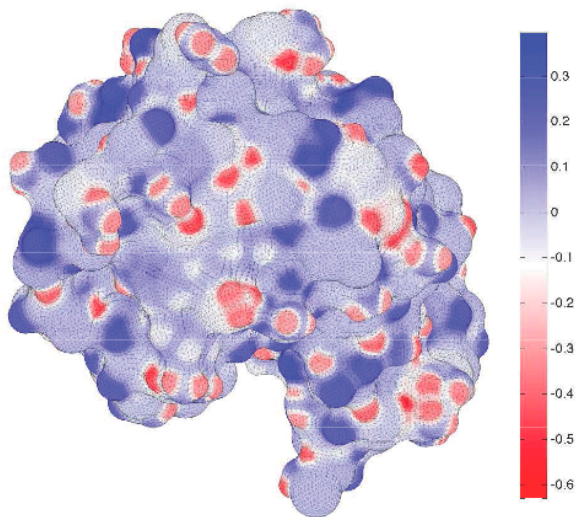
Solvation computation
can benefit from
operator simplification,
and non-Poisson models.

Solvation computation
can benefit from
operator simplification,
and non-Poisson models.

Solvation computation
can benefit from
operator simplification,
and non-Poisson models.

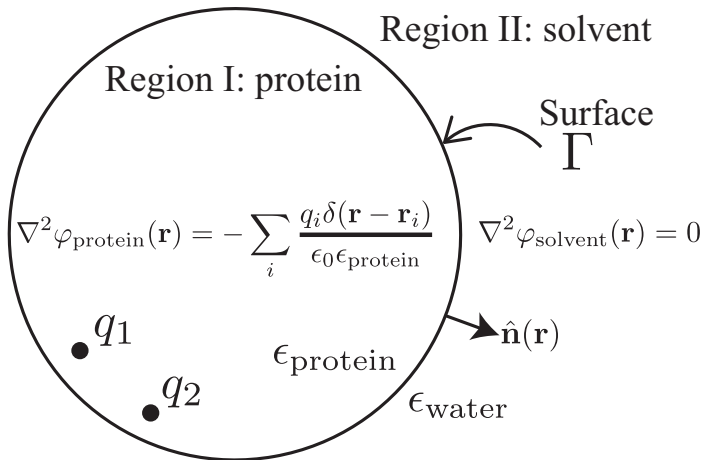
Bioelectrostatics

The Natural World



Induced Surface Charge on Lysozyme

Electrostatic Potential ϕ



We can write a Boundary Integral Equation (BIE) for the induced surface charge σ ,

$$\sigma(\vec{r}) + \hat{\epsilon} \int_{\Gamma} \frac{\partial}{\partial n(\vec{r})} \frac{\sigma(\vec{r}') d^2\vec{r}'}{4\pi\|\vec{r} - \vec{r}'\|} = -\hat{\epsilon} \sum_{k=1}^Q \frac{\partial}{\partial n(\vec{r})} \frac{q_k}{4\pi\|\vec{r} - \vec{r}_k\|}$$
$$(\mathcal{I} + \hat{\epsilon}D^*)\sigma(\vec{r}) =$$

where we define

$$\hat{\epsilon} = 2 \frac{\epsilon_I - \epsilon_{II}}{\epsilon_I + \epsilon_{II}} < 0$$

Outline

- 1 Approximating the Poisson Operator
 - Approximate Operators
 - Approximate Boundary Conditions
- 2 Improving the Poisson Operator

Problem

Boundary element discretizations of solvation:

- can be expensive to solve
- are more accurate than required by intermediate design iterations

Outline

- 1 Approximating the Poisson Operator
 - Approximate Operators
 - Approximate Boundary Conditions

Generalized Born Approximation

The pairwise energy between charges is defined by the *Still equation*:

$$G_{es}^{ij} = \frac{1}{8\pi} \left(\frac{1}{\epsilon_{II}} - \frac{1}{\epsilon_I} \right) \sum_{i,j}^N \frac{q_i q_j}{r_{ij}^2 + R_i R_j e^{-r_{ij}^2/4R_i R_j}}$$

where the *effective Born radius* is

$$R_i = \frac{1}{8\pi} \left(\frac{1}{\epsilon_{II}} - \frac{1}{\epsilon_I} \right) \frac{1}{E_i}$$

where E_i is the *self-energy* of the charge q_i , the electrostatic energy when atom i has unit charge and all others are neutral.

GB Problems

- No global potential solution, only energy
- No analysis of the error
 - For example, [Salsbury 2006](#) consists of parameter tuning
- No path for systematic improvement
 - For example, [Sigalov 2006](#) changes the model
- The same atoms have different radii in different
 - molecules,
 - solvents
 - temperatures
- **LOTS** of parameters
 - [Nina, Beglov, Roux 1997](#)

GB Problems

- No global potential so
- No analysis of the error
 - For example, [Salsbury 2006](#)
- No path for systematic improvement
 - For example, [Sigalov 2006](#)
- The same atoms have different radii
 - molecules,
 - solvents
 - temperatures
- **LOTS** of parameters
 - [Nina, Beglov, Roux 1997](#)

TABLE 2: Atomic Born Radii Derived from Solvent Electrostatic Charge Distribution Tested with Free Energy Perturbation Methods in an Explicit Solvent^a

atom	radius (Å)	
Backbone		
C	2.04	carbonyl C, peptide backbone
O	1.52	carbonyl oxygen
	2.23	peptide nitrogen
CA	2.86	all CA except Gly
CA	2.38	Gly only
Hydrogens		
H*	0.00	all hydrogens
Side Chains		
CB	2.67	all residues
CG*	2.46	Val, Ile, Arg, Lys, Met, Phe, Thr, Trp, Gln, Glu
CD*	2.44	Ile, Leu, Arg, Lys
CD, CG	1.98	Asp, Glu, Asn, Gln
CB, CG, CD	1.98	Pro only
CE*, CD*, CZ,	2.00	Tyr, Phe rings
CE*, CD*, CZ*, CH2	1.78	Trp ring only
CE	2.10	Met only
CZ, CE	2.80	Arg, Lys
OE*, OD*	1.42	Glu, Asp, Asn, Gln
OG*	1.64	Ser, Thr
OH	1.85	Tyr only
NH*, NE, NZ	2.13	Arg, Lys
NE2, ND2	2.15	Gln, Asn
NE2, ND1	2.31	His only
NE1	2.40	Trp
S*	2.00	Met, Cys

^a Patches N-term and C-term CAT, CAY: 2.06 Å. CY: 2.04 Å. OY: 1.52 Å. NT: 2.23 Å. * refers to a wild card character.

Bioelectrostatics

Mathematical Model

The *reaction* potential is given by

$$\phi^R(\vec{r}) = \int_{\Gamma} \frac{\sigma(\vec{r}') d^2\vec{r}'}{4\pi\epsilon_1 \|\vec{r} - \vec{r}'\|} = C\sigma$$

which defines G_{es} , the electrostatic part of the solvation free energy

$$\begin{aligned} \Delta G_{es} &= \frac{1}{2} \langle q, \phi^R \rangle \\ &= \frac{1}{2} \langle q, Lq \rangle \\ &= \frac{1}{2} \langle q, CA^{-1}Bq \rangle \end{aligned}$$

where

$$Bq = -\hat{\epsilon} \int_{\Omega} \frac{\partial}{\partial n(\vec{r})} \frac{q(\vec{r}') d^3\vec{r}'}{4\pi \|\vec{r} - \vec{r}'\|}$$

$$A\sigma = \mathcal{I} + \hat{\epsilon}\mathcal{D}^*$$

BIBEE

Approximate \mathcal{D}^* by a diagonal operator

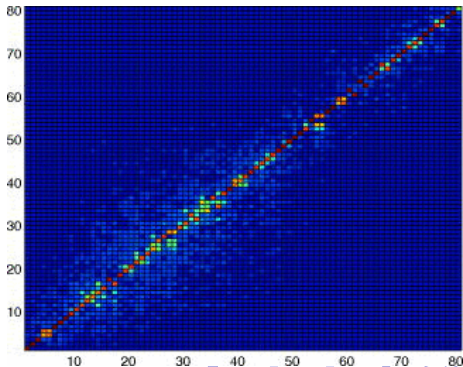
Boundary Integral-Based Electrostatics Estimation

Coulomb Field Approximation:
uniform normal field

$$\left(1 - \frac{\hat{\epsilon}}{2}\right) \sigma_{CFA} = Bq$$

Lower Bound:
no good physical motivation

$$\left(1 + \frac{\hat{\epsilon}}{2}\right) \sigma_{LB} = Bq$$

Eigenvectors: BEM $e_i \cdot e_j$ BIBEE/P

BIBEE

Approximate \mathcal{D}^* by a diagonal operator

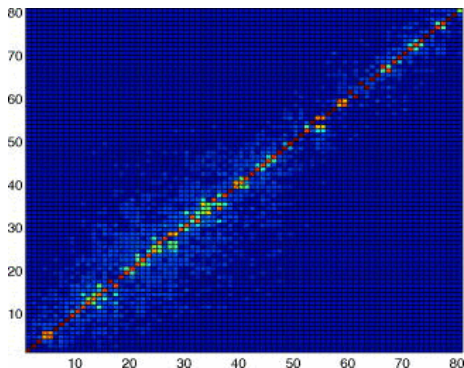
Boundary Integral-Based Electrostatics Estimation

Coulomb Field Approximation:
uniform normal field

$$\left(1 - \frac{\hat{\epsilon}}{2}\right) \sigma_{CFA} = Bq$$

Preconditioning:
consider only local effects

$$\sigma_P = Bq$$

Eigenvectors: BEM $e_i \cdot e_j$ BIBEE/P

BIBEE Bounds on Solvation Energy

Theorem: The electrostatic solvation energy ΔG_{es} has upper and lower bounds given by

$$\frac{1}{2} \left(1 + \frac{\hat{\epsilon}}{2}\right)^{-1} \langle q, CBq \rangle \leq \frac{1}{2} \langle q, CA^{-1}Bq \rangle \leq \frac{1}{2} \left(1 - \frac{\hat{\epsilon}}{2}\right)^{-1} \langle q, CBq \rangle,$$

and for spheres and prolate spheroids, we have the improved lower bound,

$$\frac{1}{2} \langle q, CBq \rangle \leq \frac{1}{2} \langle q, CA^{-1}Bq \rangle,$$

and we note that

$$|\hat{\epsilon}| < \frac{1}{2}.$$

Energy Bounds:

Proof: Bardhan, Knepley, Anitescu, JCP, **130**(10), 2008

I will break the proof into three steps,

- Replace C with B
- Symmetrization
- Eigendecomposition

shown in the following slides.

We will need the single layer operator \mathcal{S} for step 1,

$$\mathcal{S}\tau(\vec{r}) = \int \frac{\tau(\vec{r}')d^2\vec{r}'}{4\pi\|\vec{r} - \vec{r}'\|}$$

Energy Bounds: First Step

Replace C with B

The potential at the boundary Γ given by

$$\phi^{Coulomb}(\vec{r}) = C^T q$$

can also be obtained by solving an exterior Neumann problem for τ ,

$$\begin{aligned} \phi^{Coulomb}(\vec{r}) &= S\tau \\ &= S(\mathcal{I} - 2\mathcal{D}^*)^{-1} \left(\frac{2}{\hat{\epsilon}} Bq \right) \\ &= \frac{2}{\hat{\epsilon}} S(\mathcal{I} - 2\mathcal{D}^*)^{-1} Bq \end{aligned}$$

so that the solvation energy is given by

$$\frac{1}{2} \langle q, CA^{-1}Bq \rangle = \frac{1}{\hat{\epsilon}} \langle S(\mathcal{I} - 2\mathcal{D}^*)^{-1} Bq, (\mathcal{I} + \hat{\epsilon}\mathcal{D}^*)^{-1} Bq \rangle$$

Energy Bounds: Second Step

Quasi-Hermiticity

Plemelj's symmetrization principle holds that

$$\mathcal{S}\mathcal{D}^* = \mathcal{D}\mathcal{S}$$

and we have

$$\mathcal{S} = \mathcal{S}^{1/2}\mathcal{S}^{1/2}$$

which means that we can define a Hermitian operator H similar to \mathcal{D}^*

$$H = \mathcal{S}^{1/2}\mathcal{D}^*\mathcal{S}^{-1/2}$$

leading to an energy

$$\frac{1}{2} \langle q, CA^{-1}Bq \rangle = \frac{1}{\hat{\epsilon}} \langle Bq, \mathcal{S}^{1/2}(\mathcal{I} - 2H)^{-1}(\mathcal{I} + \hat{\epsilon}H)^{-1}\mathcal{S}^{1/2}Bq \rangle$$

Energy Bounds: Third Step

Eigendecomposition

The spectrum of \mathcal{D}^* is in $[-\frac{1}{2}, \frac{1}{2})$, and the energy is

$$\frac{1}{2} \langle q, CA^{-1}Bq \rangle = \sum_i \frac{1}{\hat{\epsilon}} (1 - 2\lambda_i)^{-1} (1 + \hat{\epsilon}\lambda_i)^{-1} x_i^2$$

where

$$H = V\Lambda V^T$$

and

$$\vec{x} = V^T S^{1/2} Bq$$

Energy Bounds: Diagonal Approximations

The BIBEE approximations yield the following bounds

$$\frac{1}{2} \langle q, CA_{CFA}^{-1} Bq \rangle = \sum_i \frac{1}{\hat{\epsilon}} (1 - 2\lambda_i)^{-1} \left(1 - \frac{\hat{\epsilon}}{2}\right)^{-1} x_i^2$$

$$\frac{1}{2} \langle q, CA_P^{-1} Bq \rangle = \sum_i \frac{1}{\hat{\epsilon}} (1 - 2\lambda_i)^{-1} x_i^2$$

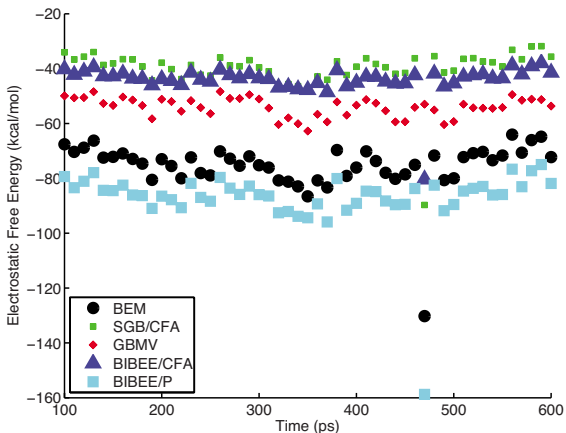
$$\frac{1}{2} \langle q, CA_{LB}^{-1} Bq \rangle = \sum_i \frac{1}{\hat{\epsilon}} (1 - 2\lambda_i)^{-1} \left(1 + \frac{\hat{\epsilon}}{2}\right)^{-1} x_i^2$$

where we note that

$$|\hat{\epsilon}| < \frac{1}{2}$$

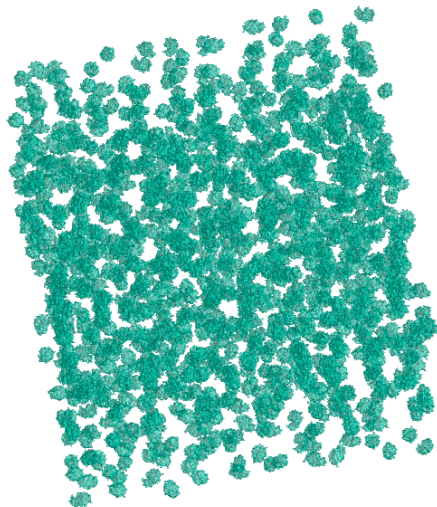
BIBEE Accuracy

Electrostatic solvation free energies of met-enkephalin structures



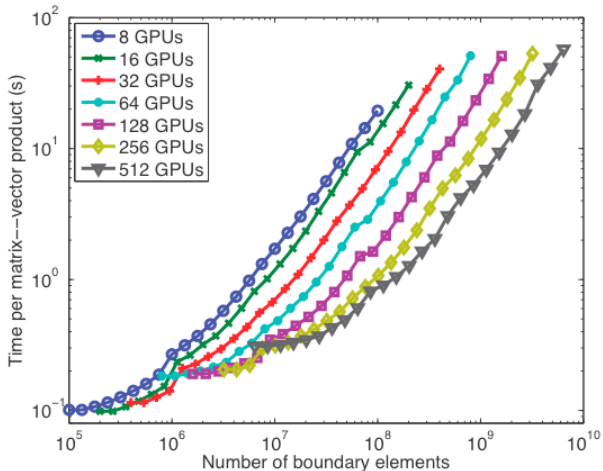
Snapshots taken from a 500-ps MD simulation at 10-ps intervals.
Bardhan, Knepley, Anitescu, JCP, 2009.

Crowded Protein Solution



Important for drug design of antibody therapies

BIBEE Scalability



Yokota, Bardhan, Knepley, Barba, Hamada, CPC, 2011.

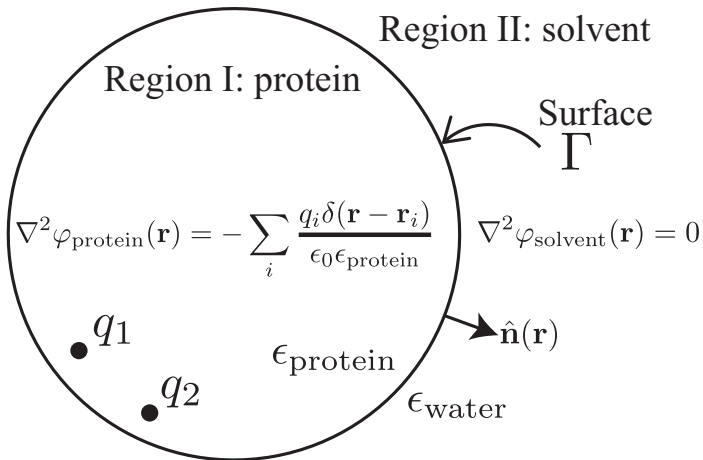
Outline

- 1 **Approximating the Poisson Operator**
 - Approximate Operators
 - **Approximate Boundary Conditions**

Bioelectrostatics

Physical Model

Electrostatic Potential ϕ



Kirkwood's Solution (1934)

The potential inside Region I is given by

$$\Phi_I = \sum_{k=1}^Q \frac{q_k}{\epsilon_1 |\vec{r} - \vec{r}_k|} + \psi,$$

and the potential in Region II is given by

$$\Phi_{II} = \sum_{n=0}^{\infty} \sum_{m=-n}^n \frac{C_{nm}}{r^{n+1}} P_n^m(\cos \theta) e^{im\phi}.$$

Kirkwood's Solution (1934)

The reaction potential ψ is expanded in a series

$$\psi = \sum_{n=0}^{\infty} \sum_{m=-n}^n B_{nm} r^n P_n^m(\cos \theta) e^{im\phi}.$$

and the source distribution is also expanded

$$\sum_{k=1}^Q \frac{q_k}{\epsilon_1 |\vec{r} - \vec{r}_k|} = \sum_{n=0}^{\infty} \sum_{m=-n}^n \frac{E_{nm}}{\epsilon_1 r^{n+1}} P_n^m(\cos \theta) e^{im\phi}.$$

Kirkwood's Solution (1934)

By applying the boundary conditions, letting the sphere have radius b ,

$$\begin{aligned}\Phi_I|_{r=b} &= \Phi_{II}|_{r=b} \\ \epsilon_I \frac{\partial \Phi_I}{\partial r} \Big|_{r=b} &= \epsilon_{II} \frac{\partial \Phi_{II}}{\partial r} \Big|_{r=b}\end{aligned}$$

we can eliminate C_{nm} , and determine the reaction potential coefficients in terms of the source distribution,

$$B_{nm} = \frac{1}{\epsilon_I b^{2n+1}} \frac{(\epsilon_I - \epsilon_{II})(n+1)}{\epsilon_I n + \epsilon_{II}(n+1)} E_{nm}.$$

Approximate Boundary Conditions

Theorem: The BIBEE boundary integral operator approximations

$$A_{CFA} = \mathcal{I} \left(1 + \frac{\hat{\epsilon}}{2} \right)$$

$$A_P = \mathcal{I}$$

have an equivalent PDE formulation,

$$\epsilon_I \Delta \Phi_{CFA,P} = \sum_{k=1}^Q q_k \delta(\vec{r} - \vec{r}_k)$$

$$\frac{\epsilon_I}{\epsilon_{II}} \frac{\partial \Phi_I^C}{\partial r} \Big|_{r=b} = \frac{\partial \Phi_{II}}{\partial r} - \frac{\partial \psi_{CFA}}{\partial r} \Big|_{r=b}$$

$$\epsilon_{II} \Delta \Phi_{CFA,P} = 0$$

or

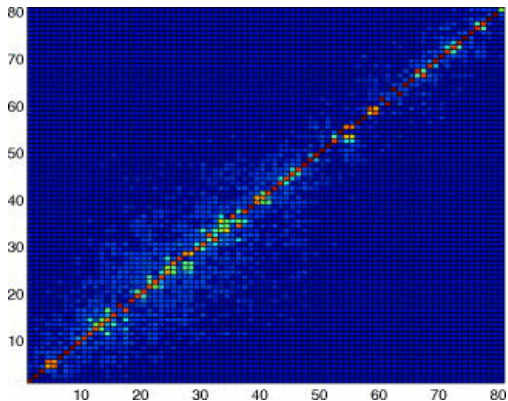
$$\Phi_I \Big|_{r=b} = \Phi_{II} \Big|_{r=b}$$

$$\frac{3\epsilon_I - \epsilon_{II}}{\epsilon_I + \epsilon_{II}} \frac{\partial \Phi_I^C}{\partial r} \Big|_{r=b} = \frac{\partial \Phi_{II}}{\partial r} - \frac{\partial \psi_P}{\partial r} \Big|_{r=b},$$

where Φ_I^C is the Coulomb field due to interior charges.

Approximate Boundary Conditions

Theorem: For spherical solute, the BIBEE boundary integral operator approximations have eigenspaces are identical to that of the original operator.



BEM eigenvector $e_i \cdot e_j$ BIBEE/P eigenvector

Proof of PDE Equivalence

Proof: Bardhan and Knepley, JCP, **135**(12), 2011.

In order to show that these PDEs are equivalent to the original BIEs,

- Start with the fundamental solution to Laplace's equation $G(r, r')$
- Note that $\int_{\Gamma} G(r, r')\sigma(r')d\Gamma$ satisfies the bulk equation and decay at infinity
- Insertion into the approximate BC gives the BIBEE boundary integral approximation

Proof of PDE Equivalence

Proof: Bardhan and Knepley, JCP, **135**(12), 2011.

In order to show that these PDEs are equivalent to the original BIEs,

- Start with the fundamental solution to Laplace's equation $G(r, r')$
- Note that $\int_{\Gamma} G(r, r')\sigma(r')d\Gamma$ satisfies the bulk equation and decay at infinity
- Insertion into the approximate BC gives the BIBEE boundary integral approximation

Proof of PDE Equivalence

Proof: Bardhan and Knepley, JCP, **135**(12), 2011.

In order to show that these PDEs are equivalent to the original BIEs,

- Start with the fundamental solution to Laplace's equation $G(r, r')$
- Note that $\int_{\Gamma} G(r, r')\sigma(r')d\Gamma$ satisfies the bulk equation and decay at infinity
- Insertion into the approximate BC gives the BIBEE boundary integral approximation

Proof of PDE Equivalence

Proof: Bardhan and Knepley, JCP, **135**(12), 2011.

In order to show that these PDEs are equivalent to the original BIEs,

- Start with the fundamental solution to Laplace's equation $G(r, r')$
- Note that $\int_{\Gamma} G(r, r')\sigma(r')d\Gamma$ satisfies the bulk equation and decay at infinity
- Insertion into the approximate BC gives the BIBEE boundary integral approximation

Proof of Eigenspace Equivalence

Proof: Bardhan and Knepley, JCP, **135**(12), 2011.

In order to show that these integral operators share a common eigenbasis,

- Note that, for a spherical boundary, \mathcal{D}^* is compact and has a pure point spectrum
- Examine the effect of the operator on a unit spherical harmonic charge distribution
- Use completeness of the spherical harmonic basis

Proof of Eigenspace Equivalence

Proof: Bardhan and Knepley, JCP, **135**(12), 2011.

In order to show that these integral operators share a common eigenbasis,

- Note that, for a spherical boundary, \mathcal{D}^* is compact and has a pure point spectrum
- Examine the effect of the operator on a unit spherical harmonic charge distribution
- Use completeness of the spherical harmonic basis

Proof of Eigenspace Equivalence

Proof: Bardhan and Knepley, JCP, **135**(12), 2011.

In order to show that these integral operators share a common eigenbasis,

- Note that, for a spherical boundary, \mathcal{D}^* is compact and has a pure point spectrum
- Examine the effect of the operator on a unit spherical harmonic charge distribution
- Use completeness of the spherical harmonic basis

Proof of Eigenspace Equivalence

Proof: Bardhan and Knepley, JCP, **135**(12), 2011.

In order to show that these integral operators share a common eigenbasis,

- Note that, for a spherical boundary, \mathcal{D}^* is compact and has a pure point spectrum
- Examine the effect of the operator on a unit spherical harmonic charge distribution
- Use completeness of the spherical harmonic basis

Proof of Eigenspace Equivalence

Proof: Bardhan and Knepley, JCP, **135**(12), 2011.

In order to show that these integral operators share a common eigenbasis,

- Note that, for a spherical boundary, \mathcal{D}^* is compact and has a pure point spectrum
- Examine the effect of the operator on a unit spherical harmonic charge distribution
- Use completeness of the spherical harmonic basis

The result does not hold for general boundaries.

Series Solutions

Note that the approximate solutions are *separable*:

$$B_{nm} = \frac{1}{\epsilon_1 n + \epsilon_2 (n+1)} \gamma_{nm}$$

$$B_{nm}^{CFA} = \frac{1}{\epsilon_2} \frac{1}{2n+1} \gamma_{nm}$$

$$B_{nm}^P = \frac{1}{\epsilon_1 + \epsilon_2} \frac{1}{n + \frac{1}{2}} \gamma_{nm}.$$

If $\epsilon_I = \epsilon_{II} = \epsilon$, both approximations are exact:

$$B_{nm} = B_{nm}^{CFA} = B_{nm}^P = \frac{1}{\epsilon(2n+1)} \gamma_{nm}.$$

Series Solutions

Note that the approximate solutions are *separable*:

$$B_{nm} = \frac{1}{\epsilon_1 n + \epsilon_2 (n + 1)} \gamma_{nm}$$

$$B_{nm}^{CFA} = \frac{1}{\epsilon_2} \frac{1}{2n + 1} \gamma_{nm}$$

$$B_{nm}^P = \frac{1}{\epsilon_1 + \epsilon_2} \frac{1}{n + \frac{1}{2}} \gamma_{nm}.$$

If $\epsilon_I = \epsilon_{II} = \epsilon$, both approximations are exact:

$$B_{nm} = B_{nm}^{CFA} = B_{nm}^P = \frac{1}{\epsilon(2n + 1)} \gamma_{nm}.$$

Asymptotics

BIBEE/CFA is exact for the $n = 0$ mode,

$$B_{00} = B_{00}^{CFA} = \frac{\gamma_{00}}{\epsilon_2},$$

whereas BIBEE/P approaches the exact response in the limit $n \rightarrow \infty$:

$$\lim_{n \rightarrow \infty} B_{nm} = \lim_{n \rightarrow \infty} B_{nm}^P = \frac{1}{(\epsilon_1 + \epsilon_2)n} \gamma_{nm}.$$

Asymptotics

BIBEE/CFA is exact for the $n = 0$ mode,

$$B_{00} = B_{00}^{CFA} = \frac{\gamma_{00}}{\epsilon_2},$$

whereas BIBEE/P approaches the exact response in the limit $n \rightarrow \infty$:

$$\lim_{n \rightarrow \infty} B_{nm} = \lim_{n \rightarrow \infty} B_{nm}^P = \frac{1}{(\epsilon_1 + \epsilon_2)n} \gamma_{nm}.$$

Asymptotics

In the limit $\epsilon_1/\epsilon_2 \rightarrow 0$,

$$\lim_{\epsilon_1/\epsilon_2 \rightarrow 0} B_{nm} = \frac{\gamma_{nm}}{\epsilon_2(n+1)}$$

$$\lim_{\epsilon_1/\epsilon_2 \rightarrow 0} B_{nm}^{CFA} = \frac{\gamma_{nm}}{\epsilon_2(2n+1)},$$

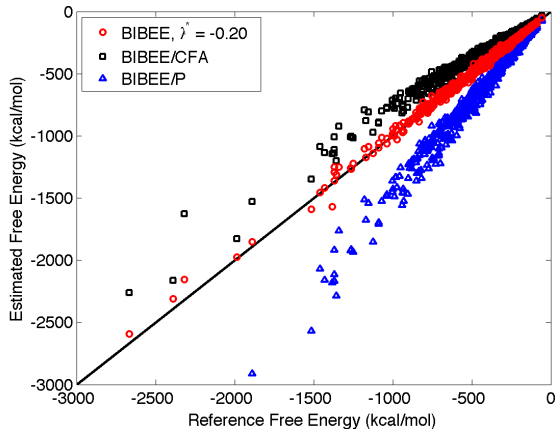
$$\lim_{\epsilon_1/\epsilon_2 \rightarrow 0} B_{nm}^P = \frac{\gamma_{nm}}{\epsilon_2(n + \frac{1}{2})},$$

so that the approximation ratios are given by

$$\frac{B_{nm}^{CFA}}{B_{nm}} = \frac{n+1}{2n+1}, \quad \frac{B_{nm}^P}{B_{nm}} = \frac{n+1}{n + \frac{1}{2}}.$$

Improved Accuracy

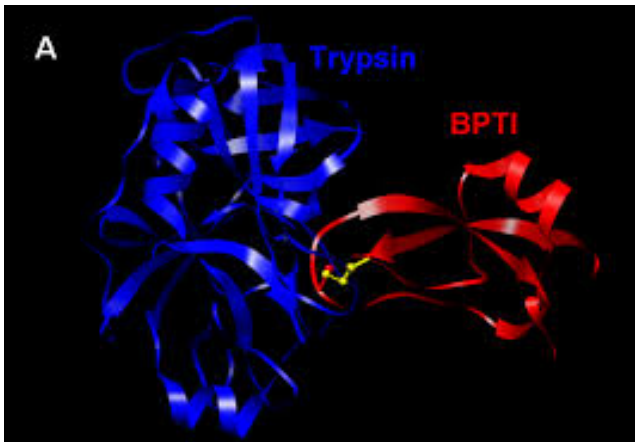
BIBEE/I interpolates between BIBEE/CFA and **BIBEE/P**



Bardhan, Knepley, JCP, 2011.

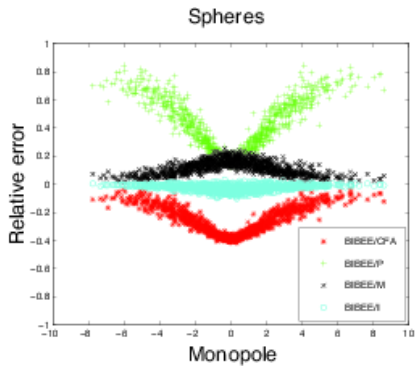
Basis Augmentation

We examined the more complex problem of **protein-ligand binding** using trypsin and bovine pancreatic trypsin inhibitor (BPTI), using *electrostatic component analysis* to identify residue contributions to binding and molecular recognition.

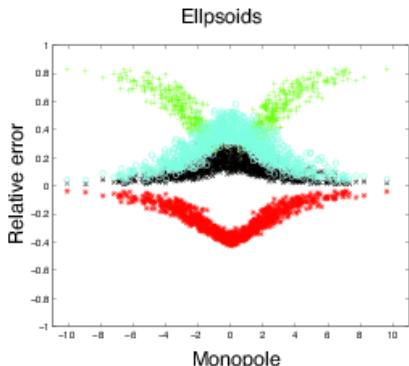


Basis Augmentation

Looking at an ensemble of synthetic proteins, we can see that **BIBEE/CFA** becomes more accurate as the monopole moment increases, and **BIBEE/P** more accurate as it decreases. **BIBEE/I** is accurate for spheres, but must be extended for ellipsoids.



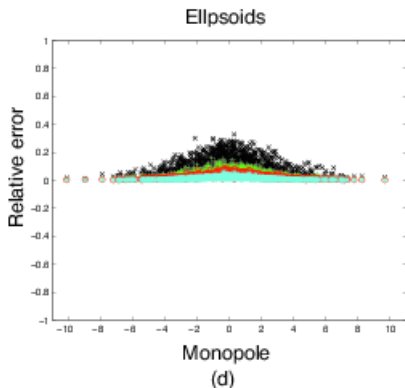
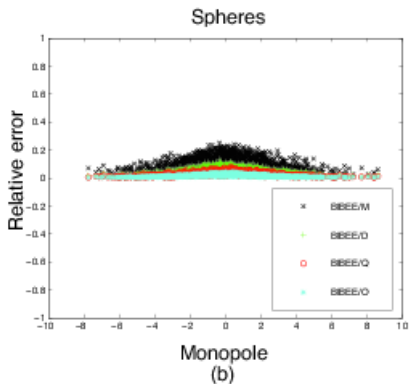
(a)



(b)

Basis Augmentation

For ellipses, we add a few low order multipole moments, up to the octopole, to recover 5% accuracy for all synthetic proteins tested.



Resolution

Boundary element discretizations of the solvation problem:

- can be expensive to solve
 - **Bounding the electrostatic free energies associated with linear continuum models of molecular solvation**, Bardhan, Knepley, Anitescu, JCP, 2009
- are more accurate than required by intermediate design iterations
 - **Analysis of fast boundary-integral approximations for modeling electrostatic contributions of molecular binding**, Kreienkamp, et al., Molecular-Based Mathematical Biology, 2013

Resolution

Boundary element discretizations of the solvation problem:

- can be expensive to solve
 - **Bounding the electrostatic free energies associated with linear continuum models of molecular solvation**, Bardhan, Knepley, Anitescu, JCP, 2009
- are more accurate than required by intermediate design iterations
 - **Analysis of fast boundary-integral approximations for modeling electrostatic contributions of molecular binding**, Kreienkamp, et al., Molecular-Based Mathematical Biology, 2013

Resolution

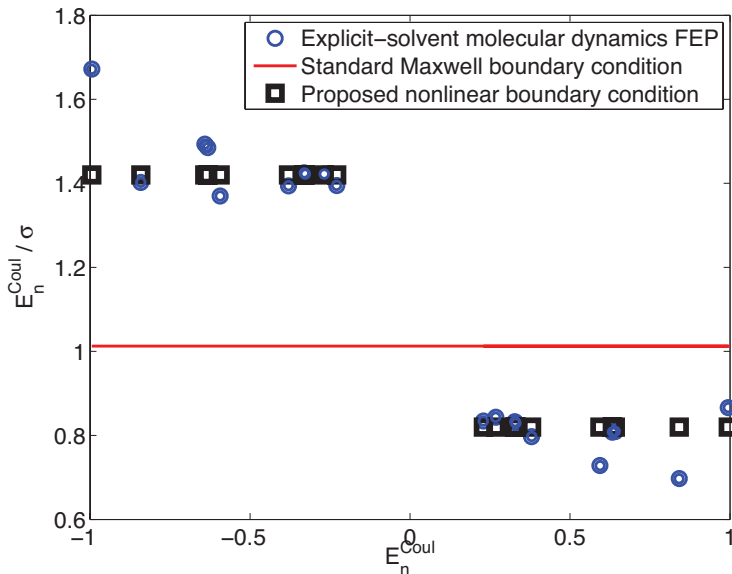
Boundary element discretizations of the solvation problem:

- can be expensive to solve
 - **Bounding the electrostatic free energies associated with linear continuum models of molecular solvation**, Bardhan, Knepley, Anitescu, JCP, 2009
- are more accurate than required by intermediate design iterations
 - **Analysis of fast boundary-integral approximations for modeling electrostatic contributions of molecular binding**, Kreienkamp, et al., Molecular-Based Mathematical Biology, 2013

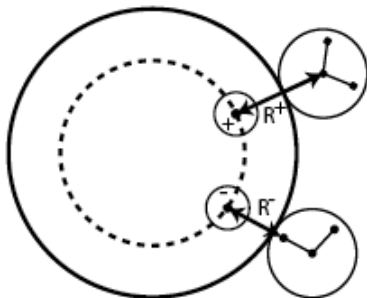
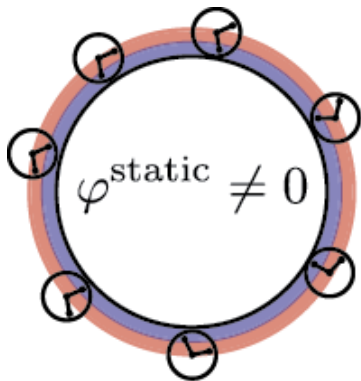
Outline

- 1 Approximating the Poisson Operator
- 2 Improving the Poisson Operator**

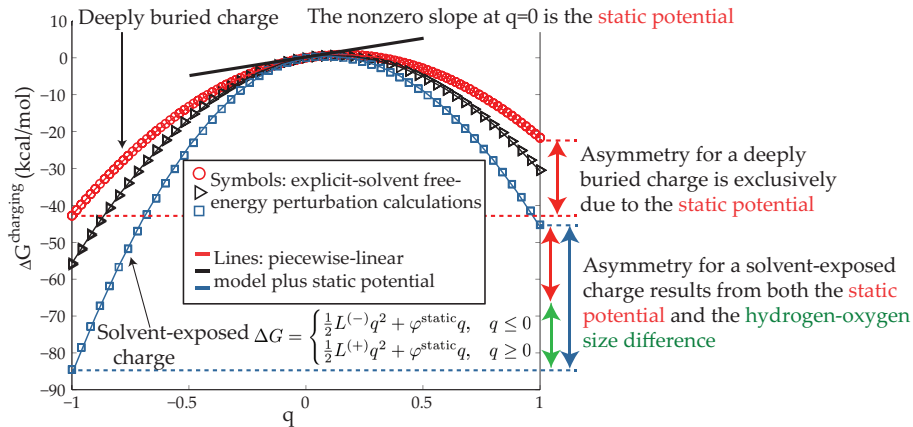
Origins of Electrostatic Asymmetry



Origins of Electrostatic Asymmetry



Origins of Electrostatic Asymmetry



Main Idea

Solvation-Layer Interface Condition (SLIC)

Instead of assuming the model and energy and deriving the radii,

$$\epsilon_I \frac{\partial \Phi_I}{\partial n} = \epsilon_{II} \frac{\partial \Phi_{II}}{\partial n}$$

Main Idea

Solvation-Layer Interface Condition (SLIC)

assume the energy and radii and derive the model.

$$(\epsilon_I - \Delta\epsilon h(E_n)) \frac{\partial\Phi_I}{\partial n} = (\epsilon_{II} - \Delta\epsilon h(E_n)) \frac{\partial\Phi_{II}}{\partial n}$$

Main Idea

Solvation-Layer Interface Condition (SLIC)

Using our correspondence with the BIE form,

$$\left(\mathcal{I} + h(\mathbf{E}_n) + \hat{\epsilon} \left(-\frac{1}{2}\mathcal{I} + \mathcal{D}^* \right) \right) \sigma = \hat{\epsilon} \sum_{k=1}^Q \frac{\partial G}{\partial n}$$

where h is a diagonal nonlinear integral operator.

SLIC

Boundary Perturbation

$$h(E_n) = \alpha \tanh(\beta E_n - \gamma) + \mu$$

where

α Size of the asymmetry

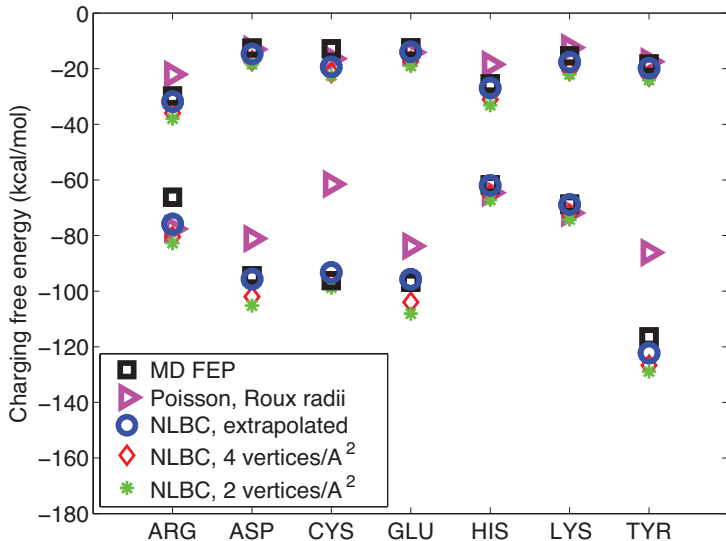
β Width of the transition region

γ The transition field strength

μ Assures $h(0) = 0$, so $\mu = -\alpha \tanh(-\gamma)$

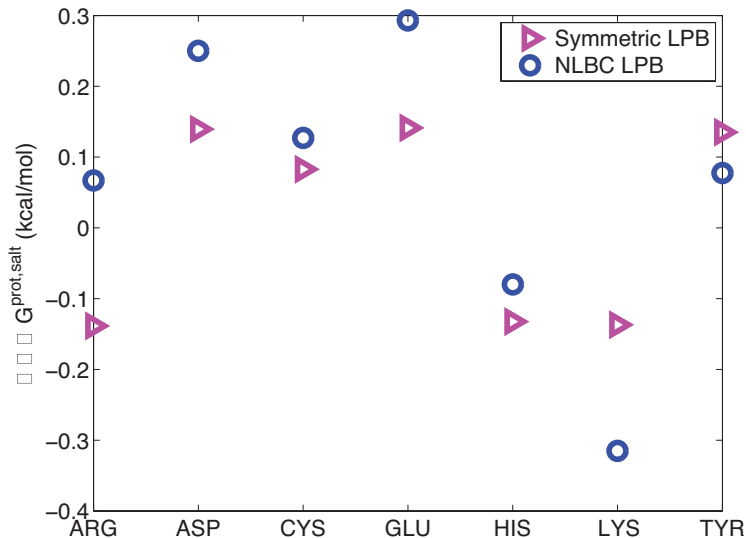
Accuracy of SLIC

Residues



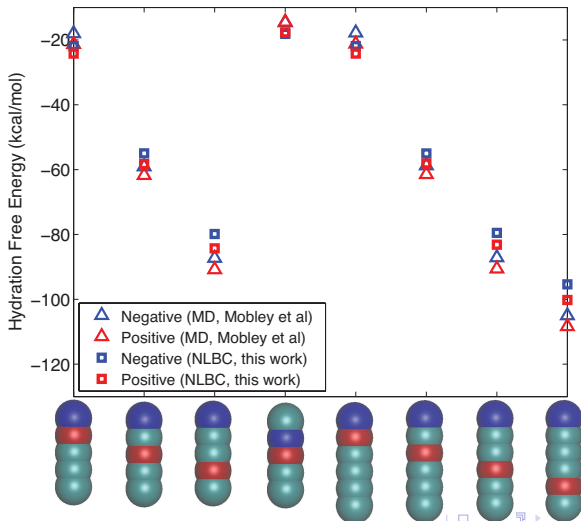
Accuracy of SLIC

Protonation



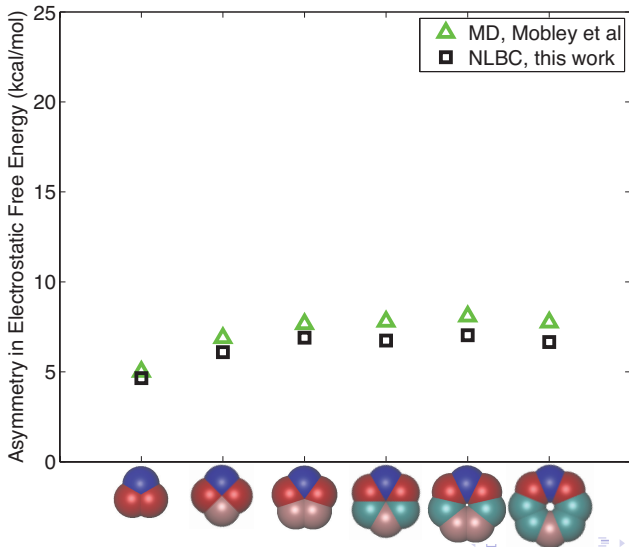
Accuracy of SLIC

Synthetic Molecules



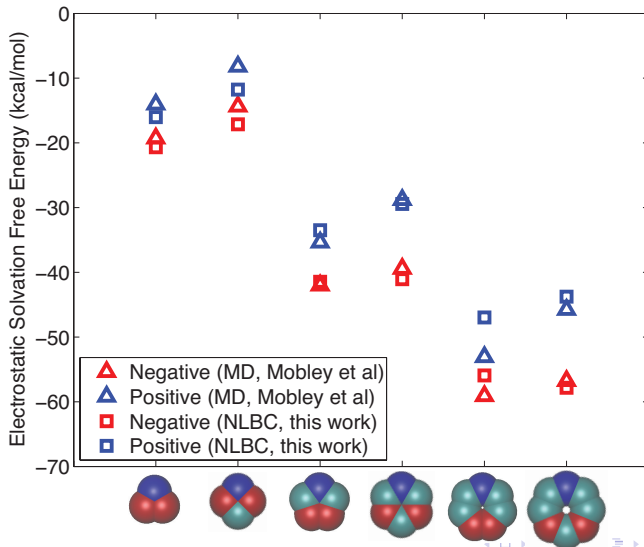
Accuracy of SLIC

Synthetic Molecules



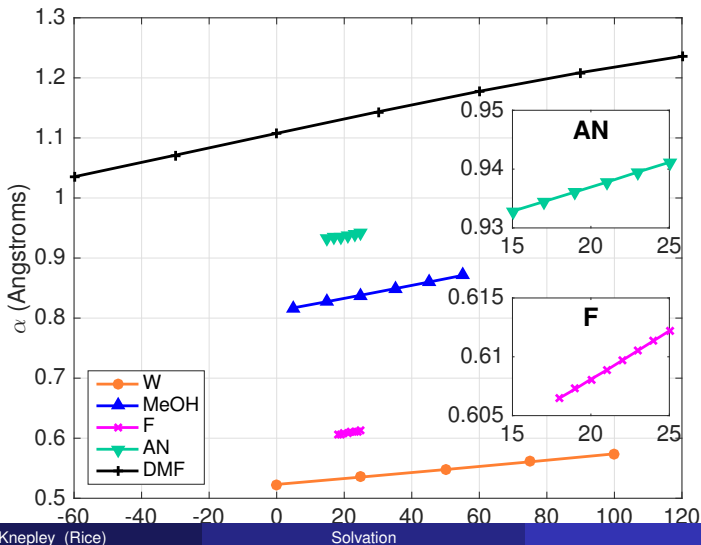
Accuracy of SLIC

Synthetic Molecules




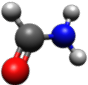

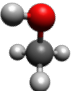


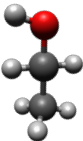
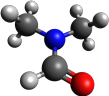
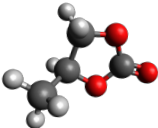
Thermodynamics

The parameters show linear temperature dependence



Model Validation

Courtesy A. Molvai Tabrizi

Water H_2O 	Formamide CH_3NO 	Dimethyl sulfoxide $\text{C}_2\text{H}_6\text{OS}$ 
Methanol CH_3OH 	Acetonitrile $\text{C}_2\text{H}_3\text{N}$ 	Nitromethane CH_3NO_2 
Ethanol $\text{C}_2\text{H}_5\text{OH}$ 	Dimethyl formamide $\text{C}_3\text{H}_7\text{NO}$ 	Propylene carbonate $\text{CH}_3\text{C}_2\text{H}_3\text{O}_2\text{CO}$ 

Model Validation

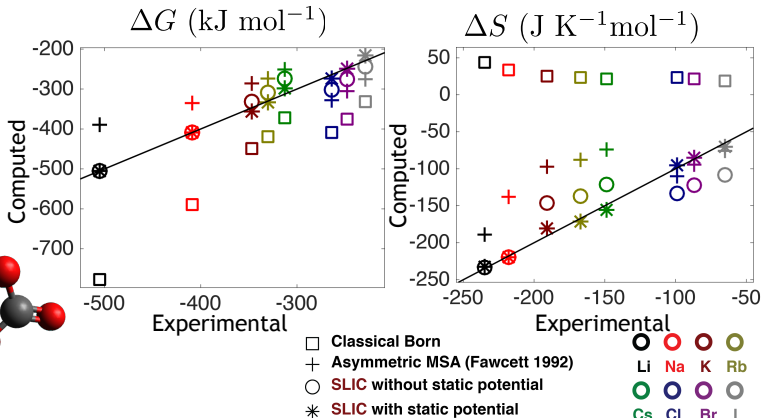
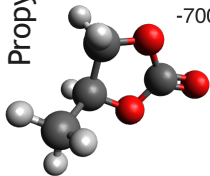
Courtesy A. Molvai Tabrizi

Solvent	r_s (Å)	$\epsilon_{out}(T)$	$\epsilon_{out}(25^\circ\text{C})$
W	1.370	$\epsilon_{out} = 87.740 - 4.0008e-1 T + 9.398e-4 T^2 - 1.410e-6 T^3$	78.3
MeOH	1.855	$\log_{10} \epsilon_{out} = \log_{10}(32.63) - 2.64e-3(T - 25)$	32.6
EtOH	2.180	$\log_{10} \epsilon_{out} = \log_{10}(24.30) - 02.70e-3 (T - 25)$	24.3
F	1.725	$\epsilon_{out} = 109 - 7.2e-1 (T - 20)$	105.4
AN	2.135	$\epsilon_{out} = 37.50 - 1.6e-1 (T - 20)$	36.7
DMF	2.585	$\epsilon_{out} = 42.04569 - 2.204448e-1 T + 7.718531e-4 T^2 - 1.000389e-6 T^3$	37.0
DMSO	2.455	$\epsilon_{out} = -60.5 + (5.7e4/(T + 273.15)) - (7.5e6/(T + 273.15)^2)$	46.3
NM	2.155	$\log_{10} \epsilon_{out} = \log_{10}(35.8) - 1.89e-3 (T - 30)$	36.6
PC	2.680	$\epsilon_{out} = 56.670738 + 2.58431e-1 T - 7.7143e-4 T^2$	62.6

Model Validation

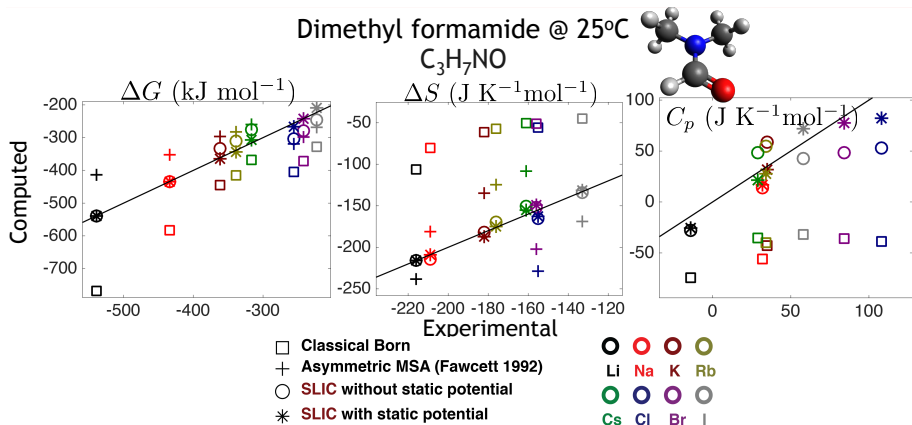
Courtesy A. Molvai Tabrizi

Propylene carbonate
 $\text{CH}_3\text{C}_2\text{H}_3\text{O}_2\text{CO}$



Model Validation

Courtesy A. Molvai Tabrizi



Model Validation

Courtesy A. Molvai Tabrizi

A. Molavi Tabrizi, M.G. Knepley, and J.P. Bardhan,
Generalising the mean spherical approximation as a multiscale, nonlinear boundary condition at the solute-solvent interface,
Molecular Physics (2016).

Thermodynamic Predictions

Courtesy A. Molvai Tabrizi

Solvent	Ion	ΔG (kJ mol ⁻¹)	ΔS (J K ⁻¹ mol ⁻¹)	C_p (J K ⁻¹ mol ⁻¹)
W	F ⁻	-430 (-429)	-67 (-115)	-86 (-45)
MeOH	Rb ⁺	-326(-319)	-178 (-175)	55
	F ⁻	-415	-116	-79 (-131)
EtOH	Rb ⁺	-319 (-313)	-197 (-187)	128
	F ⁻	-405	-145	-153 (-194)
F	Rb ⁺	-340 (-334)	-135 (-130)	27
	F ⁻	-418	-128	36 (28)
AN	F ⁻	-390	-192	147
DMF	F ⁻	-389	-230	105
DMSO	Rb ⁺	-348 (-339)	-151 (-180)	32
	F ⁻	-400	-160	186(60)
NM	Rb ⁺	-324 (-318)	-186 (-183)	19
	F ⁻	-391	-182	95(71)
PC	F ⁻	-394	-149	67

Experimental Data in Parentheses

Thermodynamic Predictions

Courtesy A. Molvai Tabrizi

A. Molavi Tabrizi, S. Goossens, M.G. Knepley, and
J.P. Bardhan,

*Predicting solvation thermodynamics with dielectric
continuum theory and a solvation-layer interface
condition (SLIC).*

Submitted to Journal of Physical Chemistry Letters
(2016).

Where does SLIC fail?

- Large packing fraction
 - No charge oscillation or overcharging
 - Could use CDFT
- No dielectric saturation
 - Could be possible with different function
- No long range correlations
 - Use nonlocal dielectric

Future Work

- More complex solutes
- Mixtures
- Integration into community code
 - Psi4, QChem, APBS
- Integrate into conformational search
 - Kavrakis Lab at Rice

Thank You!

<http://www.caam.rice.edu/~mk51>